THE JOURNAL OF BIOLOGICAL CHEMISTRY VOL. 287, NO. 40, pp. 33836–33846, September 28, 2012

Structural Basis of Rev1-mediated Assembly of a Quaternary Vertebrate Translesion Polymerase Complex Consisting of Rev1, Heterodimeric Polymerase (Pol) ζ, and Pol κ*

Received for publication, June 23, 2012, and in revised form, July 17, 2012 Published, JBC Papers in Press, August 2, 2012, DOI 10.1074/jbc.M112.394841

Jessica Wojtaszek[‡1], Chul-Jin Lee[‡1], Sanjay D'Souza[§], Brenda Minesinger[§], Hyungjin Kim[¶2], Alan D. D'Andrea[¶], Graham C. Walker[§], and Pei Zhou[‡3]

From the [‡]Department of Biochemistry, Duke University, Medical Center, Durham, North Carolina 27710, the [§]Department of Biology, Massachusetts Institute of Technology, Cambridge, Massachusetts 02139, and the [¶]Department of Radiation Oncology, Dana-Farber Cancer Institute, Boston, Massachusetts 02215

Background: Translesion synthesis in mammalian cells is achieved by sequential actions of insertion and extension polymerases.
Results: We determined the Rev1-Pol ζ-Pol κ complex structure and verified the binding interface with *in vivo* studies.
Conclusion: Mammalian insertion and extension polymerases could cooperate within a megatranslesion polymerase complex nucleated by Rev1.
Significance: The Rev1-Pol ζ interface is a target for developing novel cancer therapeutics.

DNA synthesis across lesions during genomic replication requires concerted actions of specialized DNA polymerases in a potentially mutagenic process known as translesion synthesis. Current models suggest that translesion synthesis in mammalian cells is achieved in two sequential steps, with a Y-family DNA polymerase (κ, η, ι, or Rev1) inserting a nucleotide opposite the lesion and with the heterodimeric B-family polymerase ζ, consisting of the catalytic Rev3 subunit and the accessory Rev7 subunit, replacing the insertion polymerase to carry out primer extension past the lesion. Effective translesion synthesis in vertebrates requires the scaffolding function of the C-terminal domain (CTD) of Rev1 that interacts with the Rev1-interacting region of polymerases κ, η, and ι and with the Rev7 subunit of polymerase ζ. We report the purification and structure determination of a quaternary translesion polymerase complex consisting of the Rev1 CTD, the heterodimeric Pol ζ complex, and the Pol κ Rev1-interacting region. Yeast two-hybrid assays were employed to identify important interface residues of the translesion polymerase complex. The structural elucidation of such a quaternary translesion polymerase complex encompassing both insertion and extension polymerases bridged by the Rev1 CTD provides the first molecular explanation of the essential scaffolding function of Rev1 and highlights the Rev1 CTD as a promising target for developing novel cancer therapeutics to suppress translesion synthesis. Our studies support the notion that vertebrate insertion and extension polymerases could structurally cooperate within a megatranslesion polymerase complex (translesionsome) nucleated by Rev1 to achieve efficient lesion bypass without incurring an additional switching mechanism.

Timely replication of genetic information prior to mitosis is essential for maintaining genome stability. Although high fidelity DNA replicases are proficient at duplicating genomic DNA, they are intolerant of most forms of DNA lesions continuously generated in large numbers by endogenous cellular processes and environmental genotoxic agents (1). Despite the presence of highly efficient DNA repair processes in cells, a small number of lesions inevitably evade the surveillance of sophisticated repair machinery and block the progression of high fidelity replicases during genomic replication, resulting in arrested replication forks and generation of single-stranded replication gaps. Both of these events contribute to genome instability and pose a serious challenge for cell viability. In order to resolve stalled replication forks and gaps at lesion sites, cells have evolved a special set of DNA polymerases that are capable of directly replicating across DNA lesions (translesion synthesis) at the cost of replication fidelity (2, 3).

Two distinct translesion synthesis pathways have been genetically defined in *Saccharomyces cerevisiae*; one involves relatively error-free bypass of TT cyclobutane pyrimidine dimers by Pol[4] η (Rad30), and the other one involves Rev1 and the heterodimeric Pol ζ, consisting of the catalytic Rev3 subunit and the accessory Rev7 subunit, that are responsible for error-prone translesion synthesis across lesions caused by UV and a variety of other DNA-damaging agents. Indeed, *REV1*, *REV3*, and *REV7* were the first translesion polymerase genes identified based on mutations that resulted in significantly reduced muta-

* This work was supported, in whole or in part, by NIGMS, National Institutes of Health (NIH), Grant GM-079376 (to P. Z.); NIEHS, NIH, Grant ES-015818 (to G. C. W.); and NIH Grants R01DK43889, R37HL52725, and RC4DK090913 (to A. D. D.). This work was also supported by the Stewart Trust Foundation (to P. Z.) and an American Cancer Society research professorship (to G. C. W.).
The atomic coordinates and structure factors (code 4FJO) have been deposited in the Protein Data Bank, Research Collaboratory for Structural Bioinformatics, Rutgers University, New Brunswick, NJ (http://www.rcsb.org/).
[1] Both authors contributed equally to this work.
[2] Recipient of the Leukemia and Lymphoma Society Career Development Fellowship.
[3] To whom correspondence should be addressed. Tel.: 919-668-6409; Fax: 919-684-8885; E-mail: peizhou@biochem.duke.edu.

[4] The abbreviations used are: Pol, polymerase; CTD, C-terminal domain; RIR, Rev1-interacting region; mRev1, mRev3, and mRev7, mouse Rev1, Rev3, and Rev7, respectively; TEV, tobacco etch virus; PDB, Protein Data Bank.

genicity (nonmutable or "reversionless" phenotype) (4, 5), highlighting their essential roles in the mutagenic branch of translesion synthesis in yeast.

A greater number of translesion polymerases have been identified in mammalian cells, including four Y-family translesion polymerases, Pol κ, Pol η, Pol ι, and Rev1, and one B-family translesion polymerase, Pol ζ (2, 3). These polymerases account for the vast majority of translesion synthesis activities in mammalian cells, and they cooperatively achieve efficient lesion bypass in two sequential steps (6). In the first step, one of the four Y-family polymerases, each with its own distinct lesion specificity, inserts a nucleotide(s) opposite the DNA lesion. After nucleotide incorporation, the insertion polymerase is "switched" to an extension polymerase for primer extension past the lesion site. Although Pol η may specifically contribute to primer extension past TT cyclobutane pyrimidine dimers, substantial evidence supports the notion that primer extension past lesion sites is predominantly carried out by the Rev1-Pol ζ complex in mammalian cells (7).

Rev1, which is conserved from yeast to humans, is a unique member of the Y-family polymerases. It was the first enzymatically characterized translesion polymerase and possesses a deoxycytidyltransferase activity (8). Two key findings have led to the suggestion of a "second function" of Rev1 that is separate from its catalytic activity (9). First was the observation that Rev1 was required for bypassing a T-T(6–4) UV photoproduct independent of its catalytic activity. Second was the discovery that the nonmutable phenotype of the *S. cerevisiae rev1-1* mutant is caused by a mutation outside the catalytic domain that does not impair Rev1 deoxycytidyltransferase activity. Indeed, further experimentation has shown that mutation of the catalytic residue of Rev1 did not affect the levels of mutagenesis induced by a wide range of DNA-damaging agents (10, 11), except for causing a change of mutation spectrum, arguing that the non-catalytic role of Rev1 in translesion synthesis is to serve as an essential scaffolding protein to mediate the assembly of translesion polymerase complexes in response to DNA damage.

The scaffolding function of Rev1 in vertebrates is critically dependent on its C-terminal domain of ~100 amino acids (11), which has been shown to bind insertion polymerases κ, η, and ι through their Rev1-interacting region (RIR) (12–15) and extension polymerase ζ through its Rev7 subunit (12, 13, 16). Rev1 interaction is required for the protective role of Pol κ against benzo[*a*]pyrene in mammalian cells, and it promotes Pol η-mediated suppression of spontaneous mutations in human cells (17, 18). Although the interactions between the Rev1 CTD and the RIRs of Y-family polymerases κ, η, and ι are only found in vertebrates (15), the Rev1 CTD-Pol ζ interaction is evolutionarily conserved from yeast to humans, highlighting the essential role of the Rev1-Pol ζ interaction in translesion synthesis. Consistent with this notion, the Rev1 CTD is required for effective DNA damage tolerance in mammalian cells, and mutations of the Rev1 CTD display a profound defect in translesion synthesis with significantly reduced damage-induced mutagenesis in yeast (11, 19). Despite the rapid progress in our understanding of the non-catalytic role of the Rev1 CTD in translesion synthesis, the molecular basis of its scaffolding function has remained poorly understood until recently.

We and others have recently reported the solution structures of the mouse and human Rev1 CTD and their complexes with the RIR peptides of Pol κ and Pol η (20, 21). Using yeast two-hybrid assays, we have also mapped the Rev1 surface responsible for interaction with the Rev7 subunit of Pol ζ. Our previous studies show that the Pol κ RIR and Rev7 bind to two neighboring but non-overlapping surfaces of the Rev1 CTD. In this work, we present evidence that the Rev1 CTD simultaneously binds to Pol ζ and the Pol κ RIR and report the crystal structure of the quaternary Rev1 CTD-Pol ζ-Pol κ RIR complex. Yeast two-hybrid assays have been used to verify the Rev1 CTD-Pol ζ binding interface and to identify a set of residues important for complex formation. Alteration of a representative residue that affects the Rev1-Rev7 interaction in yeast two-hybrid assays also largely inactivates Rev1 function in the chicken DT40 cell line, indicating that the observed interaction is relevant in the context of full-length Rev1 and Pol ζ in vertebrate cells that have suffered DNA damage *in vivo*. Our studies present the first molecular details of the long speculated "second" and non-catalytic function of the Rev1 CTD and reveal an unexpected solution to the "switching" mechanism in the current model of two-step translesion synthesis. Because Rev1-Pol ζ-dependent translesion synthesis is a major factor in promoting cancer cell survival and generating cancer drug resistance after chemotherapy, our studies also provide important structural insights for developing novel cancer therapeutics to improve the outcome of chemotherapy.

EXPERIMENTAL PROCEDURES

Molecular Cloning and Protein Purification—The mouse Rev1 (mRev1) CTD constructs contained 115 residues (positions 1135–1249) for NMR studies or 100 residues (positions 1150–1249) for crystallographic studies. The mRev1 CTD constructs were cloned into a modified pMAL-C2 vector (New England BioLabs) to yield His_6-MBP-tagged protein with a TEV site between MBP and the Rev1 CTD. The mouse Pol κ RIR of residues 560–577 was cloned into modified pET vectors (EMD Biosciences) to produce a GB1-Pol κ RIR fusion protein connected by a three-residue linker (Gly-Ser-Glu) for NMR titration studies and a His_{10}-GB1-tagged protein with a TEV site between GB1 and the RIR for crystallography studies. The mouse Pol ζ was produced by co-expression of the Rev7-interacting fragment of mRev3 (residues 1844–1895) and full-length mRev7 containing an R124A mutation using a pCDF-Duet-1 vector (Novagen). The mRev3 fragment was cloned into the first multiple cloning site, and mRev7 containing an N-terminal His_8 tag was cloned into the second cloning site.

The His_6-MBP-tagged mRev1 CTD was overexpressed in GW6011 *Escherichia coli* cells, induced with 0.1 mM isopropyl 1-thio-β-D-galactopyranoside at 18 °C for 18 h after the A_{600} reached 0.4. The mouse Pol κ RIR constructs were overexpressed in BL21(DE3)STAR *E. coli* cells, induced with 1 mM isopropyl 1-thio-β-D-galactopyranoside at 37 °C for 6 h after the A_{600} reached 0.5. The GB1-Pol κ RIR fusion protein was purified using an IgG affinity column according to the standard protocol (GE Healthcare) followed by size exclusion chromatography. For crystallography studies, the mRev1 CTD-Pol κ RIR complex was prepared by co-lysing *E. coli* cells overex-

pressing the MBP-TEV-Rev1 CTD and GB1-TEV-Pol κ RIR and co-purified by Ni^{2+}-nitrilotriacetic acid affinity chromatography. After TEV digestion to remove the His_6-MBP tag from the mRev1 CTD and the His_{10}-GB1 tag from mouse Pol κ RIR, the mRev1 CTD-Pol κ RIR complex was further purified by size exclusion chromatography. The mRev3 and mRev7 proteins were co-expressed in BL21(DE3)STAR *E. coli* cells, induced with 1 mM isopropyl 1-thio-β-D-galactopyranoside at 37 °C for 6 h after A_{600} reached 0.5. After lysing cells using a French pressure cell, the Rev3/7 complex was purified by Ni^{2+}-nitrilotriacetic acid affinity chromatography and size exclusion chromatography.

The final crystallization sample containing the quaternary complex of the Rev1 CTD, Rev3/7, and Pol κ RIR complex was prepared by passing the protein mixture of Rev3/7 with a slight molar excess amount of the Rev1 CTD-Pol κ RIR complex through a size exclusion column (HiPrep 26/60 Sephacryl S-200 HR, GE Healthcare).

NMR Spectroscopy—Isotopically labeled Rev1 CTD samples were obtained by growing *E. coli* cells in M9 medium containing either H_2O or a high percentage of D_2O (90%), using [^{15}N]NH_4Cl and [^{13}C]glucose as the sole nitrogen and carbon sources. NMR experiments were conducted using an Agilent INOVA 800-MHz spectrometer at 25 °C. Resonance assignments of the free Rev1 CTD (1135–1249) were obtained using standard three-dimensional triple-resonance experiments (22). NMR titration was carried out by recording HSQC spectra of the ^{2}H/^{15}N-labeled Rev1 CTD in the presence of increasing molar ratios of unlabeled GB1-Pol κ RIR or Pol ζ (Rev3/7). The spectrum of the ^{15}N-labeled Rev1 CTD in the presence of equal molar ratios of both GB1-Pol κ RIR and Pol ζ was also recorded to establish the formation of the quaternary Rev1 CTD-Rev3/7-Pol κ RIR complex.

Crystallization and Structure Determination—The quaternary Rev1 CTD-Rev3/7-Pol κ RIR complex used for crystallography studies contained 0.9 mM protein in a buffer of 25 mM HEPES, pH 7.2, 100 mM KCl, and 2 mM tris(2-carboxyethyl)-phosphine. Rhombic-faced polyhedron crystals were obtained using the sitting drop vapor diffusion method at 4 °C in drops containing 1.6 μl of the quaternary protein complex and 0.7 μl of well solution consisting of 0.1 M Tris, pH 8.5, and 1.5 M ammonium dihydrogen phosphate. The crystals were cryoprotected by soaking in mother liquor containing 20% glycerol (v/v) before flash-freezing. Diffraction data were collected at 100 K (λ = 1.000 Å) on the 22-BM beamline at the SERCAT at Argonne National Laboratory and processed with HKL2000 (23). Molecular replacement using AUTOMR in the PHENIX package (24) was carried out by using two search models sequentially. The first one was the crystal structure of human Rev7 in complex with a human Rev3 fragment (PDB code 3ABE), and the second one contained the ensemble of our previously determined solution structures of the mRev1 CTD in complex with the RIR of Pol κ (PDB code 2LSJ), of which both the N- and C-terminal loops and side-chain atoms were removed to reduce potential phase bias. The final coordinate was completed by iterative cycles of model building (COOT) and refinement (PHENIX) (24, 25).

Yeast Two-hybrid Assays—Protein-protein interactions in the yeast two-hybrid system were performed in the PJ69-4A strain of yeast (26). The mRev1 CTD (residues 1150–1249) and mRev7 harboring the previously described R124A substitution (27) were cloned into the pGAD-C1 (GAL4 activation domain) and pGBD-C1 (GAL4 DNA-binding domain) plasmids marked with leucine and tryptophan, respectively. The assay was performed by growing strains harboring the two plasmids in 3 ml of medium lacking leucine and tryptophan for 2 days at 30 °C and spotting 5 μl of cells on selective medium plates lacking leucine and tryptophan (−LW) and on medium also lacking adenine and histidine (−AHLW) to score positive interactions. Interactions were scored after 3 days of growth at 30 °C. Site-directed mutations were generated using the QuikChange protocol (Stratagene) and verified by sequencing.

DT40 Cell Culture and Transfection—Chicken DT40 cells were grown at 39.5 °C in RPMI medium supplemented with 10% fetal calf serum and 1% chicken serum. To generate stable transfectants, 30 μg of plasmid DNA was digested overnight with the restriction enzyme MluI. After ethanol precipitation, the linearized DNA was electroporated into ~1 × 10^7 *rev1* DT40 cells using the Gene Pulser apparatus (Bio-Rad) at 550 V, 25 μFD. Stable clones were selected after 1 week of growth in 2 mg/ml G418 (Sigma).

Plasmid DNA and Site-directed Mutagenesis—The cDNA encoding mREV1 was cloned into the pEGFP-C3 vector (Clontech). Site-directed mutations were generated using the QuikChange protocol (Stratagene) and verified by sequencing.

Immunoblot Analysis and Antibodies—For immunoblot analysis, cells were lysed in Lysis Buffer (1% Nonidet P-40, 300 mM NaCl, 0.2 mM EDTA, 50 mM Tris, pH 7.5), supplemented with a protease inhibitor mixture (Roche Applied Science), resolved by NuPAGE (Invitrogen) gels, transferred to nitrocellulose membranes, and detected with anti-GFP (JL-8, Clontech) and anti-β-actin (Cell Signaling) antibodies using the enhanced chemiluminescence system (Western Lightning, PerkinElmer Life Sciences).

DT40 Cytotoxicity Assay—For survival assays, 1.5 × 10^4 of cells were exposed to various concentrations of cisplatin (*cis*-diammineplatinum(II) dichloride; Sigma) for 72 h at 39.5 °C. Cell viability was determined using the Cell Titer-Glo luminescent cell viability assay (Promega) according to the manufacturer's instructions.

RESULTS

Formation of a Quaternary Translesion Polymerase Complex Involving the Rev1 CTD, Heterodimeric Pol ζ, and the Pol κ RIR—Our previous structural and biochemical studies of the mRev1 CTD have revealed two distinct and non-overlapping binding surfaces on the Rev1 CTD that separately mediate its interactions with the Rev7 subunit of mouse Pol ζ and the RIR peptide of mouse Pol κ. In order to investigate whether the Rev1 CTD is capable of forming a quaternary complex consisting of Rev1, Pol ζ, and Pol κ in solution, we titrated the mouse Rev1 CTD (residues 1135–1249) individually and sequentially with the Pol κ RIR as a GB1 fusion protein and a core Pol ζ complex, consisting of the Rev7-interacting fragment of Rev3 (residues 1844–1895) and a R124A mutation of mouse Rev7 that has

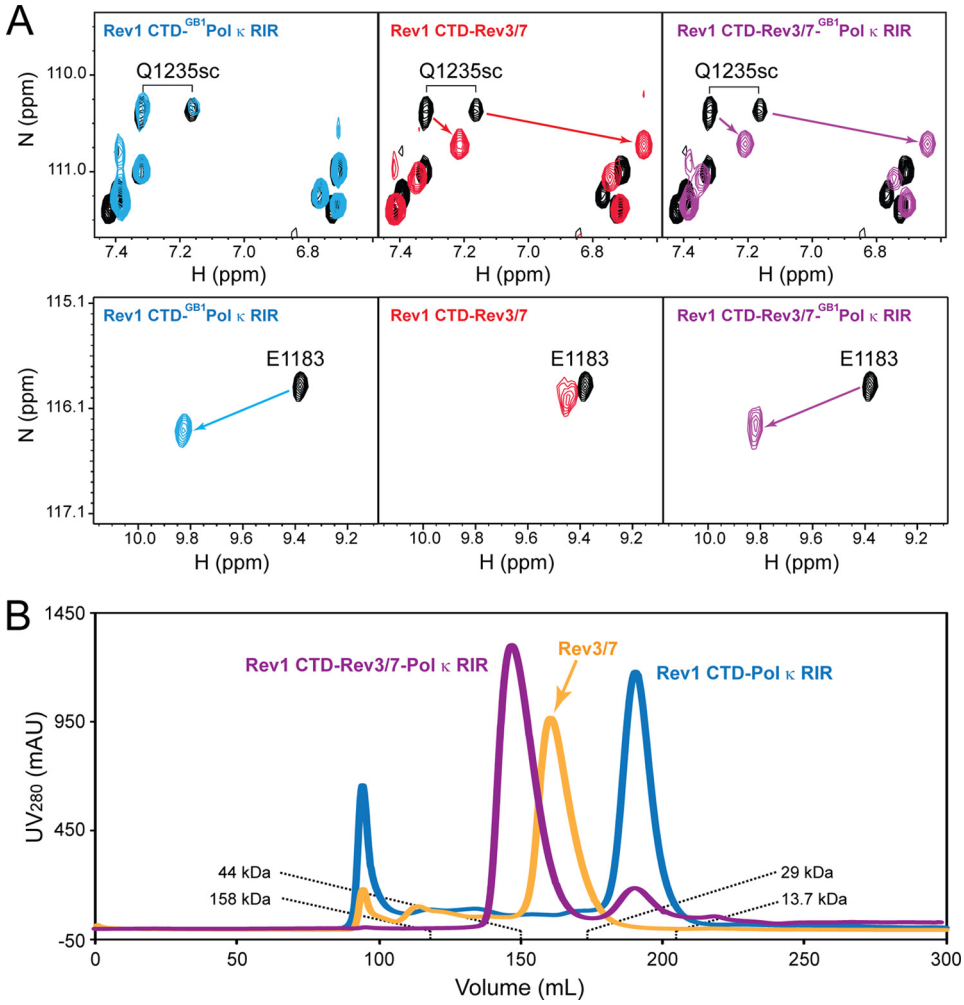

FIGURE 1. **Formation of a quaternary complex consisting of the Rev1 CTD, Rev3/7, and Pol κ RIR.** *A*, ^{1}H-^{15}N HSQC spectra of the free Rev1 CTD (*black*) and the Rev1 CTD in the presence of an equal molar ratio of either the GB1-Pol κ RIR fusion protein (*blue*), Rev3/7 (*red*), or both (*purple*). *B*, FPLC traces of the Rev1 CTD-Rev3/7-Pol κ RIR complex (*purple*), the Rev3/7 complex (*light orange*), and the Rev1 CTD-Pol κ RIR complex (*blue*) separated using a HiPrep 26/60 Sephacryl S-200 HR column (GE Healthcare). The elution volumes of known protein standards are *labeled*.

been previously shown to enhance the monomeric form of Rev7 and promote Rev1 interaction (27, 28). Titrations of unlabeled GB1-Pol κ RIR and the Rev3/7 into the ^{15}N-labeled Rev1 CTD each caused perturbation of a subset of resonances in the slow exchange regime on the NMR time scale, indicating that both the Rev1 CTD-Pol κ RIR interaction and the Rev1 CTD-Rev3/7 interaction are tight. Although the ^{1}H-^{15}N HSQC spectrum of the Rev1 CTD-Rev3/7 complex at the equal molar ratio contains fewer number of signals compared with the free Rev1 CTD, we were able to observe a set of Rev1 CTD signals that are differentially perturbed by Pol κ RIR binding (*e.g.* the backbone resonance of Glu-1183 (*E1183*) in Fig. 1*A*) and by Rev3/7 binding (*e.g.* side-chain resonances of Gln-1235 (*Q1235*) in Fig. 1*A*). It is important to note that these signals are equally perturbed in the final spectrum of the Rev1 CTD in the presence of equal molar ratios of both Pol κ RIR and Rev3/7, and the perturbed signals overlap either with those of the Rev1 CTD-Pol κ RIR complex or with the Rev1 CTD-Rev3/7 complex but not with signals from the free Rev1 CTD (*right panels* in Fig. 1*A*). This result is consistent with the formation of a quaternary Rev1 CTD-Rev3/7-Pol κ RIR complex in solution but is incompatible with co-existence of the ternary Rev1 CTD-Rev3/7 complex and the binary Rev1-Pol κ RIR complex because in the latter scenario, Rev1 CTD signals selectively perturbed by Pol κ binding but unperturbed by Rev/37 binding (or vice versa) would be present in both the perturbed and unperturbed forms in the final spectrum of complex mixture.

Consistent with the formation of a tightly binding quaternary Rev1-Rev3/7-Pol κ RIR complex in the slow exchange regime on the NMR time scale, such a quaternary complex is readily separated from the Rev1 CTD-Pol κ RIR complex and from the Rev3/7 complex on size exclusion chromatography (Fig. 1*B*).

Overall Structure of the Rev1-Pol ζ-Pol κ RIR Complex—After demonstrating the formation of a quaternary translesion polymerase complex consisting of the Rev1 CTD, Rev3/7, and the Pol κ RIR in solution, we went on to probe the molecular details of such a complex using x-ray crystallography. The complex structure was determined at 2.7 Å resolution by molecular replacement using the crystal structure of human Rev7 in complex with a Rev3 peptide (PDB code 3ABE) and our previously reported solution structure of the mouse Rev1 CTD-Pol κ RIR complex (PDB code 2LSJ) as search models. The final statistics are reported in Table 1.

TABLE 1
Data collection and refinement statistics

Space group	$P4_32_12$
Cell dimensions	
a, b, c (Å)	145.7, 145.7, 70.8
α, β, γ (degrees)	90.0, 90.0, 90.0
Reflections (unique/total)	20,970/199,455
Resolution range (Å)	23.98–2.72 (2.84–2.72)[a]
Completeness (%)	99.2 (96.0)
I/σ	28.7 (4.68)
R-merge (%)	8.1 (55.2)
No. of atoms	
Protein	2818
Water	131
Other molecules	46
R-factor (%)	20.0
R-free (%)	23.6
Average *B*-factor (Å^2)	
Protein	55.00
Water	59.43
Other molecules	125.18
Root mean square deviation from ideal geometry	
Bond lengths (Å)	0.007
Bond angles (degrees)	0.950
Ramachandran plot[b]	
Favored (%)	99.41
Allowed (%)	100.00
MolProbity	
All atom clash score	5.42
Clash score percentile[c]	100th

[a] Values in parentheses are for the highest resolution shell.
[b] Ramachandran plot statistics were generated using MolProbity.
[c] 100th percentile is the best among structures of comparable resolution; 0th percentile is the worst.

The formation of the Rev1 CTD-Rev3/7-Pol κ RIR complex is centrally mediated by the Rev1 CTD, with Rev7 and Pol κ RIR binding to two distinct and non-overlapping surfaces on the Rev1 CTD (Fig. 2). The Rev3 peptide, which is topologically trapped within Rev7 to form the heterodimeric Pol ζ complex, does not interact with the Rev1 CTD. Likewise, no interaction is observed between the Pol κ RIR and the Rev3/7 complex, leaving the Rev1 CTD as the essential scaffolding protein to nucleate the assembly of the quaternary Rev1-Rev3/7-Pol κ complex. Superimposition of the quaternary Rev1 CTD-Rev3/7-Pol κ complex with the previously reported crystal structure of the human Rev3/7 complex (PDB code 3ABE) and the solution structure of the mouse Rev1 CTD-Pol κ RIR complex (PDB code 2LSJ) reveals backbone root mean square deviation values of 0.4 and 0.9 Å for the Rev3/7 complex and for the Rev1 CTD-Pol κ RIR complex, respectively, suggesting that the Rev1 CTD in the Rev1-Pol κ complex and Rev7 in the Rev3/7 complex are conformationally available for interacting with each other to assemble the quaternary translesion polymerase complex.

Rev1 CTD and Its Interface with Pol κ RIR—In the quaternary complex, the Rev1 CTD adopts an atypical four-helix bundle fold consisting of mixed parallel and antiparallel helices, with α1, α2, α4, and α3 positioned in a clockwise fashion (Fig. 3*A*). In addition to this core four-helix bundle, the Rev1 CTD also contains two prominent loops, one located at the N terminus and one at the C terminus.

The N-terminal loop, which is disordered in the free mouse Rev1 CTD (Fig. 3*A*, *gray*) (20), folds into a β-hairpin over the surface area between helices α1 and α2 of the Rev1 CTD and creates a deep hydrophobic pocket to interact with Phe-566 and Phe-567, two invariant phenylalanine residues of the binding-induced Pol κ RIR helix. The observation of extensive van der Waals interactions between these two phenylalanine residues and hydrophobic residues of the Rev1 CTD from the N-terminal loop (Ala-1158 and Leu-1169), the α1 helix (Leu-1169, Leu-1170, and Trp-1173), the α1-α2 loop (Ile-1177), and the α2 helix (Val-1188) nicely supports our previously reported solution structure of the Rev1 CTD-Pol κ RIR complex (Fig. 3*B*) (20). The crystal structure, however, has revealed other hydrophilic interactions in addition to those we previously reported (*i.e.* the intramolecular hydrogen bond between the side-chain hydroxyl group of the N-helix cap Ser-565 and amide of Asp-568 within the Pol κ RIR helix as well as the intermolecular charge-charge interaction between the side chains of Lys-570 of the Pol κ RIR and Glu-1172 of the Rev1 CTD). In particular, we observed intermolecular bidentate hydrogen bonds between Asp-1184 of the Rev1 CTD and backbone amides of Phe-566 and Phe-567 of the Pol κ RIR (Fig. 3*C*). These two hydrogen bonds are strengthened by the favorable helix dipole effect, and they likely contribute to the stability of the Pol κ RIR helix in addition to providing anchoring points. Two additional intermolecular hydrogen bonds can also be detected between residues of the Rev1 CTD (Asn-1156 of the N-terminal loop and Gln-1187 of α2) and the Pol κ RIR (Arg-571 and Asp-568) (Fig. 3*C*). Because these two Pol κ residues are not conserved and their alanine substitutions do not affect the Rev1 CTD-Pol κ RIR binding affinity (17), their crystallographically observed polar interactions may not contribute significantly to the binding energy.

Heterodimeric Pol ζ Complex of Rev3 and Rev7—Rev7 is a member of the HORMA (*Ho*p1, *R*ev7, and *Ma*d2) family of proteins. The most thoroughly studied member of this family, Mad2 co-exists in two distinct conformations (open and closed states) in solution and only shifts to the closed state after binding to a ligand, such as MBP1 (29). The Rev7 conformation captured in the quaternary complex corresponds to the closed state of Mad2 (Fig. 4*A*), similar to that in the previously reported structure of the Rev3/7 complex (27).

The central β-sheet of Rev7 consists of five antiparallel β-strands, including β6, β4, β5, β8″, and β8′, arranged from left to right, leaving the edge of β6 available for interaction with its ligand, the invaded β1 strand of Rev3. The β1 strand of Rev3 is flanked by a small strand (β7′) of Rev7, which sandwiches the Rev3 strand between β6 and β7′ of Rev7, further expanding the central β-sheet of Rev7 to the left. On the back side of the central β-sheet lies a layer of helices (αA, αB, αC, and αD), with αA and αC sandwiched between the central β-sheet and a small β-sheet consisting of two small antiparallel β-strands (β2 and β3). The short β7′ strand flanking Rev3 is connected at its N terminus via a short α-helix (αD) to β6 of the central β-sheet and at the C terminus, through a 3_{10} helix and a "seat belt" loop extending across the central β-sheet to connect with β8′ located at the far end of the β-sheet.

In addition to interacting with the central β-sheet of Rev7 through backbone hydrogen bonds of its invaded β1 strand, Rev3 further interacts with Rev7 through an extensive set of hydrophobic residues (Fig. 4, *B* and *C*). In particular, Leu-1875 and Pro-1877 of Rev3 protrude into the core of Rev7 and inter-

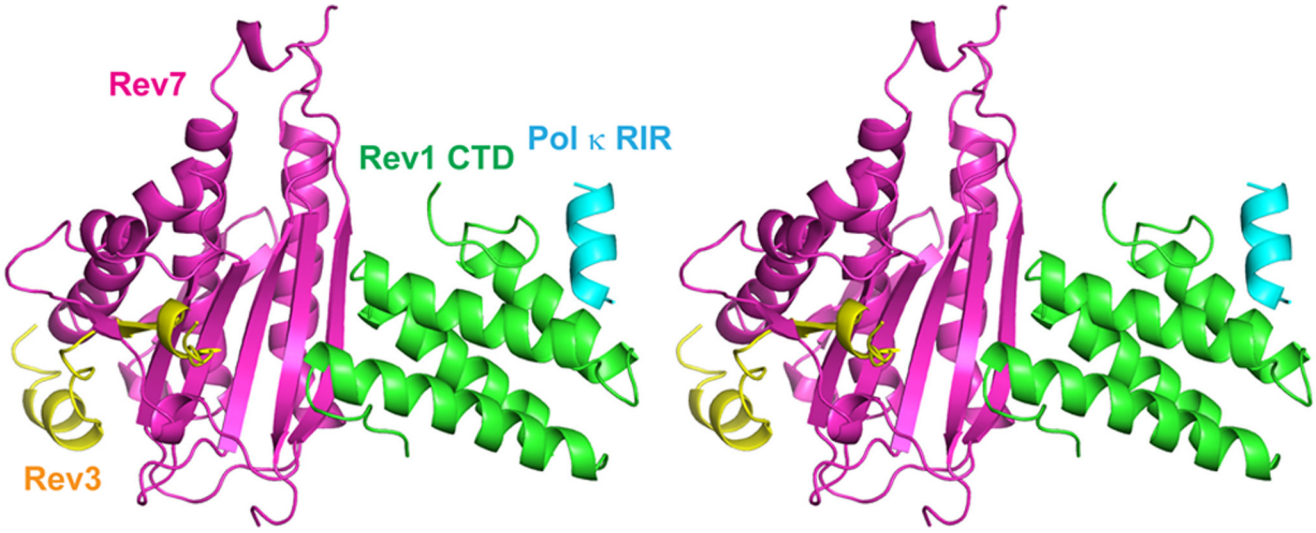

FIGURE 2. **Structure of the quaternary Rev1 CTD-Rev3/7-Pol κ RIR complex.** *Ribbon diagrams* of the complex are shown in *stereo view* and are *colored* with the Rev1 CTD in *green*, Rev3 in *yellow*, Rev7 in *purple*, and the Pol κ RIR in *cyan*.

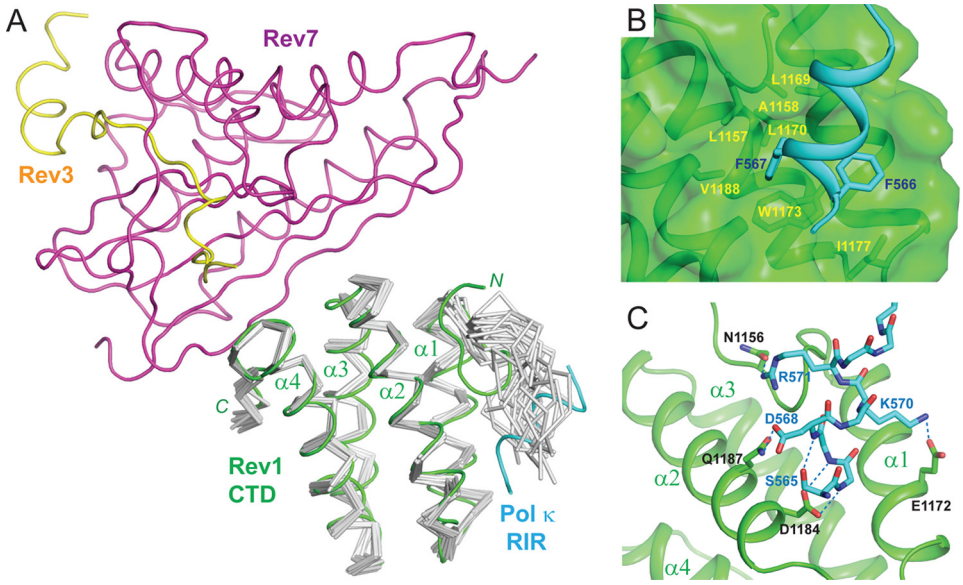

FIGURE 3. **The Rev1 CTD-Pol κ RIR interface.** *A*, structure of the Rev1 CTD-Rev3/7-Pol κ RIR complex superimposed with the NMR ensemble of the free Rev1 CTD (PDB ID: 2LSG). Components of the quaternary complex are *colored*, with the Rev1 CTD in *green*, Pol κ RIR in *cyan*, Rev7 in *purple*, and Rev3 in *yellow*. The NMR ensemble of the free Rev1 CTD is shown in Cα traces and *colored gray*. *B*, hydrophobic interactions between the Rev1 CTD and Pol κ RIR. *C*, hydrophilic interactions between the Rev1 CTD and Pol κ RIR.

act with Rev7 residues that pack the αD and αB helices against the central β-sheet of Rev7 from the back side. On the front side of the Rev7 central β-sheet, Ile-1874, Lys-1876, and Leu-1878 of the β1 strand of Rev3 form extensive interactions with Rev7 residues to anchor the β7′ strand, the 3_{10} helix, and the following seat belt loop. The residues C-terminal to the inserted β1 strand of the Rev3 fragment form an extended loop followed by a short α-helix, with the helix fitting into a shallow groove defined by the termini of αA and αB helices and the β2 and β3 strands of Rev7 (Fig. 4*C*). Hydrophobic residues of both the extended loop (Pro-1881 and Pro-1882) and C-terminal helix (Ile-1887, Leu-1888, and Leu-1891) of Rev3 form extensive van der Waals contacts with nearby Rev7 residues and are required for high affinity Rev3-Rev7 interaction (27).

Interaction of the Rev1 CTD and Rev7—The closed conformation of Rev7, stabilized by its interaction with Rev3, leaves the front face of the central β-sheet open for binding to the Rev1 CTD. The Rev1 CTD-Rev7 interaction is mediated by a combination of hydrophobic and hydrophilic residues (Fig. 5). In particular, side chains of Leu-186 and Pro-188, located on the front side of the β8′ strand of Rev7, project from the central β-sheet and wedge into a deep and narrow hydrophobic pocket on the Rev1 CTD defined by Leu-1201 and Leu-1204 from α3, Leu-1238 from α4, and Tyr-1242 and Leu-1246 from the C-terminal tail of the Rev1 CTD (Fig. 5, *A* and *B*). In addition, Tyr-202 from the neighboring β8″ strand of Rev7 touches the edge of the hydrophobic pocket on the Rev1 CTD and forms van der Waals contacts with Leu-1201 and Tyr-1242 of the Rev1 CTD.

Such a core set of hydrophobic interactions are flanked by two extensive hydrogen bond networks (Fig. 5, *C* and *D*). At the center of the first hydrogen bond network, Gln-200 of Rev7 emanates from the N terminus of the β8″ strand and reaches

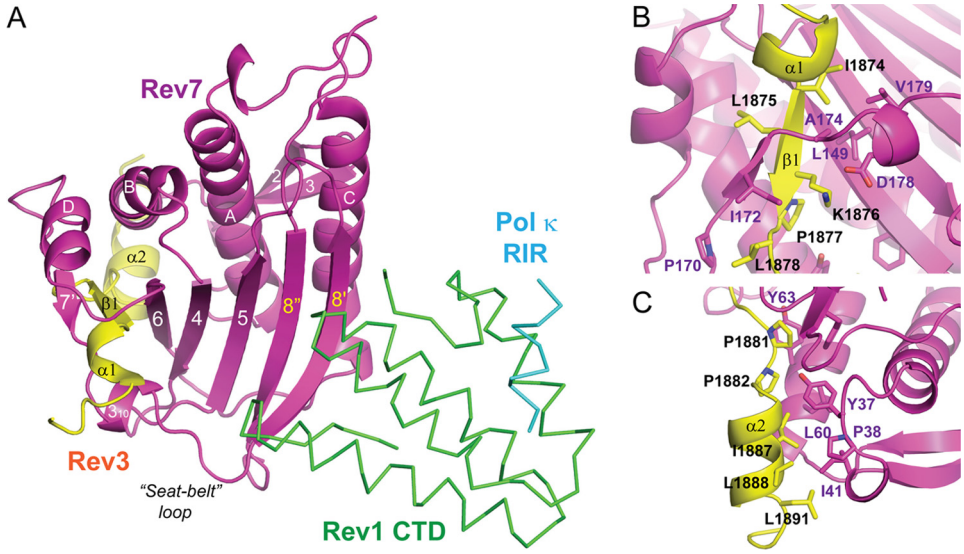

FIGURE 4. **The Rev3/7 interface.** *A*, overall structure of the Rev3/7 complex in the quaternary Rev1 CTD-Rev3/7-Pol κ RIR complex. Rev3 and Rev7 are shown in a *ribbon diagram*, and the Rev1 CTD and Pol κ RIR are shown in *Cα traces*. *B*, Rev3-Rev7 binding interface encompassing the N-terminal α1 helix and the β1 strand of Rev3. *C*, Rev3-Rev7 interface encompassing the C-terminal α2 helix and the loop connecting the β1 strand and the α2 helix of Rev3.

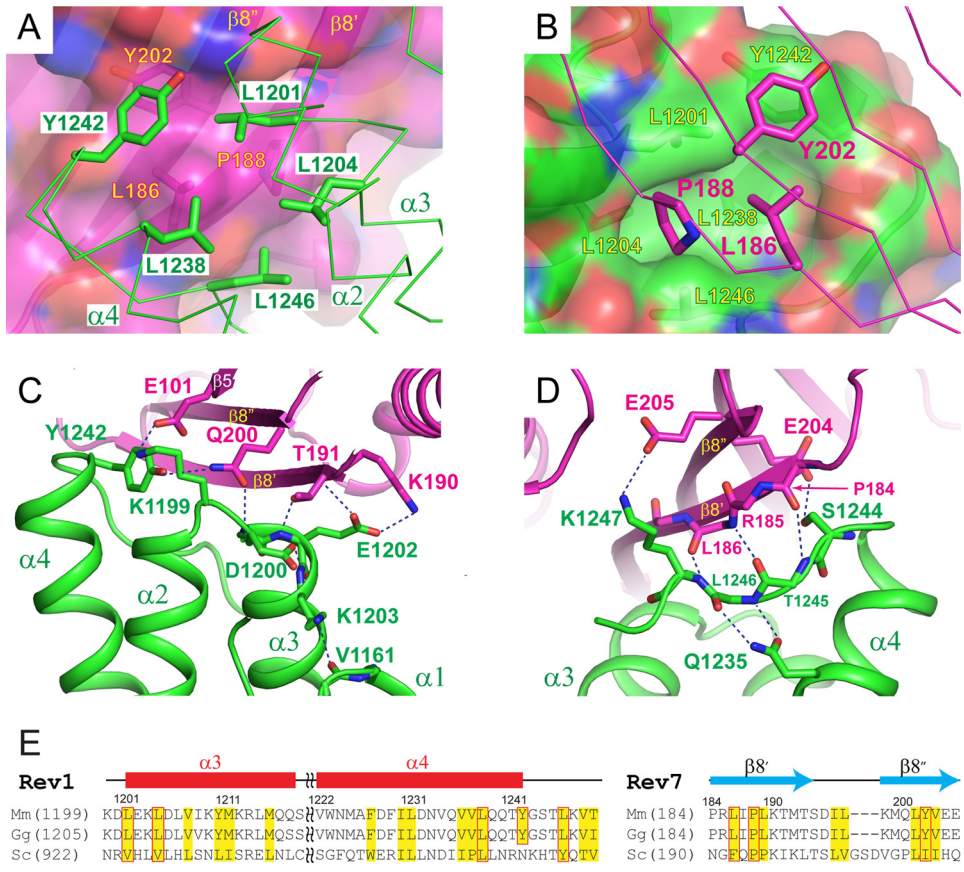

FIGURE 5. **The Rev1 CTD-Rev7 interface.** *A*, hydrophobic interactions between the Rev1 CTD and Rev7. Rev7 residues are *labeled* in *yellow*, and Rev1 residues are *labeled* in *green*. *B*, *opposite view* of *A*, illustrating the central hydrophobic pocket of the Rev1 CTD that accommodates Pro-188 and Leu-186 of Rev7. Rev7 residues are *labeled* in *purple*, and Rev1 residues are *labeled* in *yellow*. *C* and *D*, hydrophilic interactions between the Rev1 CTD and Rev7, with *C* showing interactions centered at the α2-α3 loop of the Rev1 CTD and *D* showing interactions centered at the C-terminal tail of the Rev1 CTD. *E*, sequence alignment of the Rev1 CTD and Rev7 from mouse (*Mus musculus*; *Mm*), chicken (*Gallus gallus*; *Gg*), and yeast (*S. cerevisiae*; *Sc*). Conserved hydrophobic residues are *colored yellow*. Hydrophobic residues important for the Rev1-Rev7 interaction are *boxed* in *red*.

toward the gap among the N terminus of α3 and C terminus of α4 and the following C-terminal tail of the Rev1 CTD. The side chain of Gln-200 of Rev7 forms two hydrogen bonds with the Rev1 CTD, one interacting with the backbone amide group of Leu-1201 to anchor the α3 helix and the other one interacting with the hydroxyl group of the Tyr-1242 side chain to fix its conformation as part of the hydrophobic pocket on the Rev1 CTD for Rev7 interaction. Mutation of Q200A completely dis-

TABLE 2
Summary of yeast two-hybrid results of perturbation of the Rev1 CTD-Rev7 interface

Amino acid changed in Rev7	Interaction with Rev1 CTD[a]	Amino acid changed in Rev1 CTD	Interaction with Rev7
WT	+	WT	+
L186A	−	Y1242A	−
L186E	−	L1246A	−
L186K	−	K1247E	−
Q200A	−		
Y202A	−		
P188A	−		
E101A	−		
E204A	−		
K190A	−		
T191A	+		
P184A	+		
P184K	+		

[a] +, growth on selective medium; −, no growth on selective medium.

rupted the Rev1-Rev7 interaction, highlighting the important contribution of the Gln-200 interactions (27) (Table 2). The Gln-200-mediated hydrogen bonds are buttressed by a salt bridge to the left, which connects Lys-1199 of the Rev1 CTD and Glu-101 from the β5 strand of Rev7 and constrains the orientation of the α2-α3 loop of Rev1, and an exquisite set of hydrogen bonds to the right that secure the α3 helix of the Rev1 CTD to Rev7. The observed polar interactions include hydrogen bonds between the Rev7 Thr-191 hydroxyl group and the Glu-1202 amide group of the Rev1 CTD and between the side chains of Rev7 Lys-190 and the Rev1 CTD Glu-1202. Glu-1202 of Rev1 also forms a second hydrogen bond with the amide group of Rev7 Thr-191, further enhancing the hydrogen bond network that lashes the α3 helix of the Rev1 CTD to Rev7. Although not directly involved in Rev7 interaction, Asp-1200 of Rev1 is engaged in the formation of an intramolecular hydrogen bond with the amide group of Lys-1203 and serves as a helix cap to stabilize the α3 helix. Similarly, Lys-1203 is not directly involved in the Rev7 interaction, but its side chain instead constrains the orientation of the N-terminal loop of the Rev1 CTD by forming a hydrogen bond with the carbonyl group of Val-1161. Mutations of Lys-1199, Asp-1200, Leu-1201, Glu-1202, and Lys-1203 all weakened or disrupted the Rev1-Rev7 interaction (20), consistent with the structural observation that either these Rev1 residues are directly involved in Rev7 interaction or their mutation reduces the stability of the Rev1 CTD, thus diminishing the Rev1-Rev7 binding.

The second set of the hydrogen bond network occurs exclusively around the C-terminal tail of the Rev1 CTD (Fig. 5*D*). In the Rev1-Rev7 interaction, the C-terminal tail of the Rev1 CTD extends across the β8′ strand of Rev7 and forms backbone hydrogen bonds between Thr-1245 and Lys-1247 of the Rev1 CTD and Pro-184 and Leu-186 of β8′ of Rev7 that are characteristic of the hydrogen bond patterns found in parallel β-strands. The backbone hydrogen bond contacts between Rev1 and Rev7 are flanked by two side chain-mediated hydrophilic interactions, one between the side chains of Ser-1244 at the N terminus of the Rev1 C-terminal loop and Glu-204 of Rev7 and the other between the side chains of Lys-1247 at the C-terminal end of the Rev1 loop and Glu-205 of Rev7. The interactions between the C-terminal tail of Rev1 and the β8′ strand of Rev7 are further supported by the formation of intramolecular bidentate hydrogen bonds between Gln-1235 of the α4 helix of the Rev1 CTD and the backbone of Leu-1246 of the C-terminal loop, which fasten the Rev1 C-terminal tail for interaction with Rev7. It is interesting to note that although Gln-1235 is not directly involved in the Rev7 interaction, its side-chain chemical shift is significantly perturbed upon Rev7 binding, an effect that is probably caused by its enhanced interaction with the stabilized C-terminal loop in the complex state compared with the free Rev1 CTD.

Characterization of the Rev1-Rev7 Interaction Using Yeast Two-hybrid Assays—Our previous yeast two-hybrid assays have mapped residues on the α2-α3 loop and the N terminus of the α3 helix in the Rev1 CTD as the primary site for Rev7 interaction (20). Our structural elucidation of the Rev1-Rev3/7-Pol κ RIR complex has now provided a molecular view of the Rev1-Rev7 interface that extends beyond these biochemically defined interactions. Thus, in order to obtain a detailed view of the specific contributions of individual interface residues, we expanded our yeast two-hybrid assays to evaluate the energetic contribution of these additional residues toward the Rev1-Rev7 interaction. We therefore mutated Tyr-1242, Leu-1246, and Lys-1247 in the C-terminal tail of the Rev1 CTD and probed their interaction with Rev7 using yeast two-hybrid assays. As shown in Table 2, point mutations of Y1242A, L1246A, and K1247E completely abrogated the interaction of the Rev1 CTD with Rev7, attesting to the importance of the second hydrogen bond network in the C-terminal tail of Rev1.

To more fully characterize the Rev1-Rev7 interaction, we also explored the requirement of specific amino acids of Rev7 that reside at the Rev1-Rev7 interface in promoting an interaction between these two proteins. By yeast two-hybrid analysis, mutation of amino acids that comprise the Rev7 hydrophobic patch, specifically changing Leu-186 to Ala, Lys, or Glu, Pro-188 to Ala, or Tyr-202 to Ala, completely ablated the interaction between the Rev1 CTD and Rev7 (Table 2). These results agree well with previously reported data that defined Leu-186, Tyr-202, and Gln-200 of Rev7 as "hot spots" for Rev1 binding (27). Similarly, single amino acid substitutions of most of the amino acids in Rev7 that form hydrophilic interactions with the Rev1 CTD significantly disrupt the Rev1 CTD-Rev7 binding (Table 2). For example, the specific Rev7 mutation Q200A, E101A, K190A, or E204A completely eliminated or severely diminished the interaction of Rev7 with the CTD of Rev1 (Table 2). Curiously, mutation of Thr-191 to Ala or mutation of Pro-184 to Ala or Lys (Table 2) did not disrupt the Rev1 CTD-Rev7 interaction by yeast two-hybrid assays (Table 2), suggesting that these amino acids may individually play a less critical role in the binding of Rev1. Taken together, these yeast two-hybrid data demonstrate the critical nature of the residues that define the interface between the Rev1 CTD and Rev7.

Rev1 Is Critical for DNA Damage Tolerance in Vertebrate Cells—Although we have used yeast two-hybrid assays to characterize the details of the interaction between the mouse Rev1 CTD and mouse Rev7, this approach leaves open the issue of whether these Rev1-Rev7 interactions are important in the context of full-length proteins in vertebrate cells that have been exposed to DNA damage. We therefore utilized a well characterized DT40 chicken cell line (30) to assess the ability of full-

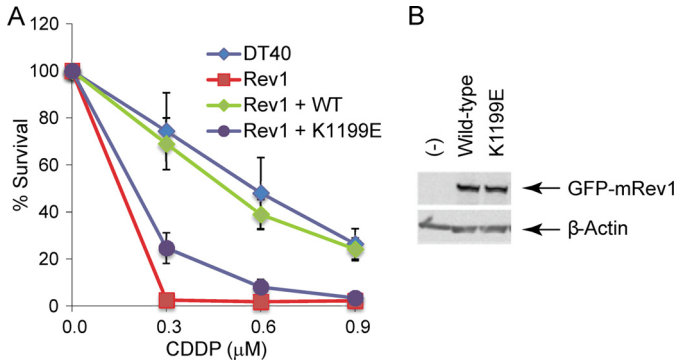

FIGURE 6. **Rev1 is critical for DNA damage tolerance in vertebrate cells.** *A*, wild-type chicken DT40 cells (*DT40*) and Rev1 deletion chicken DT40 cells (*Rev1*) harboring full-length wild-type Rev1 (*Rev1+WT*) or the K1199E mutation (*Rev1+K1199E*) were treated with the indicated doses of cisplatin (*cis*-diammineplatinum(II) dichloride), and cell viability was measured 72 h later. *B*, immunoblot analysis of lysates prepared from Rev1 deletion chicken DT40 cells (−), cells expressing full-length GFP-tagged wild-type Rev1 (*Wild-type*), and the K1199E mutation (*K1199E*) probed with an anti-GFP antibody. The same blot was probed with an anti-β-actin antibody as a loading control. *Error bars* represent standard deviation from three independent experiments.

length Rev1 harboring a representative mutation (K1199E) to complement the DNA damage sensitivity of the *rev1* cell line. Lys-1199 forms a salt bridge with Glu-101 of Rev7, and mutation of K1199E weakens the Rev1-Rev7 interaction in yeast two-hybrid assays (20). We therefore generated stable derivatives of the *rev1* cell line expressing either full-length wild-type Rev1 or the K1199E mutant, fused to an N-terminal GFP tag to follow the expression level of each protein. Although wild-type Rev1 complements the cisplatin sensitivity of the *rev1* deletion strain, the K1199E mutant failed to confer resistance to cisplatin treatment (Fig. 6*A*). We confirmed that the K1199E mutant Rev1 protein is expressed at a level similar to that of wild-type Rev1, demonstrating that the K1199E mutation does not drastically destabilize the protein (Fig. 6*B*). Taken together, these results suggest that the specific interaction between the Rev1 CTD and Rev7, characterized using yeast two-hybrid assays in our previous study (20) and in this paper, is indeed critical for the function of the Rev1-Pol ζ complex in vertebrate cells that have suffered DNA damage.

DISCUSSION

Structural Implication of the Rev1-Rev3/7-Pol κ RIR Complex in Vertebrate Translesion Synthesis—Although translesion synthesis enables timely replication of genetic information before cell division, it is an inherently error-prone process, and its employment must be tightly regulated to minimize unintended mutagenesis. The current model suggests that in mammalian cells, translesion synthesis involves multiple polymerase switches (3, 7). After replication arrest, one of the four Y-family polymerases, Pol κ, Pol η, Pol ι, or Rev1, is recruited to the stalled replication fork in replacement of the stalled replicase or to single-stranded DNA gaps for post-replicative gap filling. The insertion polymerase incorporates a nucleotide(s) opposite the lesion site, and it is then swapped with the extension polymerase, whose function is predominantly carried out by the heterodimeric Pol ζ complex in mammalian cells. After primer extension past lesion sites, Pol ζ is switched back to the high fidelity polymerase for continued DNA replication. Although the structures of several ubiquitin-binding domains have been elucidated that mediate the recruitment of insertion polymerases in response to proliferating cell nuclear antigen monoubiquitination following DNA damage (31–34), the molecular mechanism that promotes the switching from an insertion polymerase to the extension polymerase has remained a mystery.

Our previous NMR and biochemical studies have revealed two distinct and non-overlapping surface areas of the Rev1 CTD that separately mediate the interactions of the Rev1 CTD with the RIR of the insertion polymerase κ and the Rev7 subunit of Pol ζ (20). In this study, we further demonstrate that the Rev1 CTD can simultaneously bind to the RIR of Pol κ and Pol ζ to form a quaternary translesion polymerase complex. The structural observation of such a quaternary polymerase complex containing both insertion and extension polymerases suggests an elegant potential solution to the mechanism that governs the insertion-to-extension polymerase switch. The functional transition from insertion to extension could be achieved within a quaternary complex consisting of Rev1, one of three RIR-containing insertion polymerases, Pol κ, Pol η, or Pol ι, and the extension polymerase ζ. In such a complex, which we dub the translesionsome, the insertion and extension polymerases are nucleated by the Rev1 CTD to carry out efficient insertion and extension steps in translesion synthesis. In the translesionsome model, Rev1 becomes a central regulator of translesion synthesis activity because spatial or temporal variation of Rev1 would directly affect the efficiency of translesion bypass, regardless of whether or not it is dependent on proliferating cell nuclear antigen monoubiquitination (35, 36).

Evolutionarily Conserved Rev1 CTD-Rev7 Interaction—The similar genetic phenotypes caused by deficiencies of *REV1*, *REV3*, and *REV7* in yeast and mammalian cells have long implicated a functional connection of Rev1 with Rev3 and Rev7 in the Pol ζ complex (5, 30, 37, 38), and their physical interaction has been biochemically observed in yeast and vertebrate species (12, 13, 16, 39–41). Despite the biochemical verification of an evolutionarily conserved interaction between Rev1 and Rev7, there has been speculation about the structural conservation of such an interaction because Rev1 and Rev7 both show a large degree of sequence variation in yeast and vertebrates, raising the question of whether vertebrate and yeast Rev1 and Rev7 proteins use different molecular surfaces to interact with each other. Our structure of the Rev1 CTD-Rev3/7-Pol κ RIR complex has revealed a surprisingly small binding interface between Rev1 and Rev7. It is interesting to note that the Rev1 CTD residues forming the ~121 Å^3 Rev7-interacting hydrophobic pocket are highly conserved, and four of the five pocket-forming residues in mouse Rev1 (Leu-1201, Leu-1204, Leu-1238, and Leu-1246) are retained or substituted with hydrophobic residues in yeast Rev1 (Fig. 5*E*). Because these residues are also involved in the packing of the hydrophobic core of the Rev1 CTD, they are not easily identifiable as surface-exposed residues for conserved protein-protein interactions. There are an even smaller number of hydrophobic residues of Rev7 engaged in the interaction with the hydrophobic pocket of the Rev1 CTD, including only three amino acids: Leu-186 and Pro-188

located next to each other on the same side of the β8′ strand and Tyr-202 of the adjacent β8″ strand. Each of these three residues in vertebrate Rev7 is similarly conserved or replaced with an analogous hydrophobic residue in yeast Rev7 (Fig. 5*E*). In addition to these core hydrophobic interactions, we have also identified a set of backbone hydrogen bonds between the β8′ strand of Rev7 and the C-terminal loop of the Rev1 CTD that occur regardless of sequence variations. Taken together, these observations suggest that it is highly likely that the binding mode of the mouse Rev1-Rev7 interaction is structurally conserved in yeast.

Structural Implications for Cancer Therapeutics—Chemotherapy is one of the most widely employed treatment options for cancer patients. Broadly used chemotherapeutic agents, such as cyclophosphamide, cisplatin, mitomycin C, and psoralens, introduce interstrand cross-links whose repair requires Rev1 in both replication-coupled and replication-independent modes (42, 43). Studies of cancer cell lines have suggested that Rev1-mediated translesion synthesis is a major contributor to cancer cell survival and the development of drug resistance in response to cisplatin treatment (44, 45), whereas recent mouse studies have shown that knocking down the level of Rev1 delays the development of chemoresistance in drug-susceptible tumors *in vivo* (46). Additional mouse studies have shown that knocking down Rev3 sensitizes inherently drug-resistant lung adenocarcinomas to cisplatin chemotherapy (47). Taken together, these studies suggest that the Rev1-Pol ζ interface characterized in this paper may be an attractive target of the translesion synthesis system that can be exploited for development of novel cancer therapeutics.

Acknowledgment—The Rev1 DT40 clone was a generous gift from Dr. Shunichi Takeda.

REFERENCES

1. Friedberg, E. C., Walker, G. C., Siede, W., Wood, R. D., Schultz, R. A., and Ellenberger, T. (eds) (2005) *DNA Repair and Mutagenesis*, American Society for Microbiology, Washington, D. C.
2. Waters, L. S., Minesinger, B. K., Wiltrout, M. E., D'Souza, S., Woodruff, R. V., and Walker, G. C. (2009) Eukaryotic translesion polymerases and their roles and regulation in DNA damage tolerance. *Microbiol. Mol. Biol. Rev.* **73,** 134–154
3. Sale, J. E., Lehmann, A. R., and Woodgate, R. (2012) Y-family DNA polymerases and their role in tolerance of cellular DNA damage. *Nat. Rev. Mol. Cell Biol.* **13,** 141–152
4. Lemontt, J. F. (1971) Mutants of yeast defective in mutation induced by ultraviolet light. *Genetics* **68,** 21–33
5. Lawrence, C. W., Das, G., and Christensen, R. B. (1985) REV7, a new gene concerned with UV mutagenesis in yeast. *Mol. Gen. Genet.* **200,** 80–85
6. Shachar, S., Ziv, O., Avkin, S., Adar, S., Wittschieben, J., Reissner, T., Chaney, S., Friedberg, E. C., Wang, Z., Carell, T., Geacintov, N., and Livneh, Z. (2009) Two-polymerase mechanisms dictate error-free and error-prone translesion DNA synthesis in mammals. *EMBO J.* **28,** 383–393
7. Livneh, Z., Ziv, O., and Shachar, S. (2010) Multiple two-polymerase mechanisms in mammalian translesion DNA synthesis. *Cell Cycle* **9,** 729–735
8. Nelson, J. R., Lawrence, C. W., and Hinkle, D. C. (1996) Deoxycytidyl transferase activity of yeast REV1 protein. *Nature* **382,** 729–731
9. Nelson, J. R., Gibbs, P. E., Nowicka, A. M., Hinkle, D. C., and Lawrence, C. W. (2000) Evidence for a second function for *Saccharomyces cerevisiae* Rev1p. *Mol. Microbiol.* **37,** 549–554
10. Haracska, L., Unk, I., Johnson, R. E., Johansson, E., Burgers, P. M., Prakash, S., and Prakash, L. (2001) Roles of yeast DNA polymerases δ and ζ and of Rev1 in the bypass of abasic sites. *Genes Dev.* **15,** 945–954
11. Ross, A. L., Simpson, L. J., and Sale, J. E. (2005) Vertebrate DNA damage tolerance requires the C terminus but not BRCT or transferase domains of REV1. *Nucleic Acids Res.* **33,** 1280–1289
12. Guo, C., Fischhaber, P. L., Luk-Paszyc, M. J., Masuda, Y., Zhou, J., Kamiya, K., Kisker, C., and Friedberg, E. C. (2003) Mouse Rev1 protein interacts with multiple DNA polymerases involved in translesion DNA synthesis. *EMBO J.* **22,** 6621–6630
13. Ohashi, E., Murakumo, Y., Kanjo, N., Akagi, J., Masutani, C., Hanaoka, F., and Ohmori, H. (2004) Interaction of hREV1 with three human Y-family DNA polymerases. *Genes Cells* **9,** 523–531
14. Tissier, A., Kannouche, P., Reck, M. P., Lehmann, A. R., Fuchs, R. P., and Cordonnier, A. (2004) Co-localization in replication foci and interaction of human Y-family members, DNA polymerase pol η and REVl protein. *DNA Repair* **3,** 1503–1514
15. Kosarek, J. N., Woodruff, R. V., Rivera-Begeman, A., Guo, C., D'Souza, S., Koonin, E. V., Walker, G. C., and Friedberg, E. C. (2008) Comparative analysis of in vivo interactions between Rev1 protein and other Y-family DNA polymerases in animals and yeasts. *DNA Repair* **7,** 439–451
16. Murakumo, Y., Ogura, Y., Ishii, H., Numata, S., Ichihara, M., Croce, C. M., Fishel, R., and Takahashi, M. (2001) Interactions in the error-prone postreplication repair proteins hREV1, hREV3, and hREV7. *J. Biol. Chem.* **276,** 35644–35651
17. Ohashi, E., Hanafusa, T., Kamei, K., Song, I., Tomida, J., Hashimoto, H., Vaziri, C., and Ohmori, H. (2009) Identification of a novel REV1-interacting motif necessary for DNA polymerase κ function. *Genes Cells* **14,** 101–111
18. Akagi, J., Masutani, C., Kataoka, Y., Kan, T., Ohashi, E., Mori, T., Ohmori, H., and Hanaoka, F. (2009) Interaction with DNA polymerase η is required for nuclear accumulation of REV1 and suppression of spontaneous mutations in human cells. *DNA Repair* **8,** 585–599
19. D'Souza, S., Waters, L. S., and Walker, G. C. (2008) Novel conserved motifs in Rev1 C terminus are required for mutagenic DNA damage tolerance. *DNA Repair* **7,** 1455–1470
20. Wojtaszek, J., Liu, J., D'Souza, S., Wang, S., Xue, Y., Walker, G. C., and Zhou, P. (2012) Multifaceted recognition of vertebrate Rev1 by translesion polymerases ζ and κ. *J. Biol. Chem.* **287,** 26400–26408
21. Pozhidaeva, A., Pustovalova, Y., D'Souza, S., Bezsonova, I., Walker, G. C., and Korzhnev, D. M. (2012) NMR structure and dynamics of the C-terminal domain from human Rev1 and its complex with Rev1 interacting region of DNA polymerase η. *Biochemistry* **51,** 5506–5520
22. Cavanagh, J., Fairbrother, W. J., Palmer, A. G., 3rd, Skelton, N. J., and Rance, M. (2007) *Protein NMR Spectroscopy: Principles and Practice*, 2nd Ed., Elsevier Academic Press, Burlington, MA
23. Otwinowski, Z., and Minor, W. (1997) Processing of x-ray diffraction data collected in oscillation mode. *Methods Enzymol.* **276,** 307–326
24. Adams, P. D., Grosse-Kunstleve, R. W., Hung, L. W., Ioerger, T. R., McCoy, A. J., Moriarty, N. W., Read, R. J., Sacchettini, J. C., Sauter, N. K., and Terwilliger, T. C. (2002) PHENIX. Building new software for automated crystallographic structure determination. *Acta Crystallogr. D Biol. Crystallogr* **58,** 1948–1954
25. Emsley, P., and Cowtan, K. (2004) Coot. Model-building tools for molecular graphics. *Acta Crystallogr. D Biol. Crystallogr.* **60,** 2126–2132
26. James, P., Halladay, J., and Craig, E. A. (1996) Genomic libraries and a host strain designed for highly efficient two-hybrid selection in yeast. *Genetics* **144,** 1425–1436
27. Hara, K., Hashimoto, H., Murakumo, Y., Kobayashi, S., Kogame, T., Unzai, S., Akashi, S., Takeda, S., Shimizu, T., and Sato, M. (2010) Crystal structure of human REV7 in complex with a human REV3 fragment and structural implication of the interaction between DNA polymerase ζ and REV1. *J. Biol. Chem.* **285,** 12299–12307
28. Hara, K., Shimizu, T., Unzai, S., Akashi, S., Sato, M., and Hashimoto, H. (2009) Purification, crystallization, and initial x-ray diffraction study of human REV7 in complex with a REV3 fragment. *Acta Crystallogr. Sect. F Struct. Biol. Cryst. Commun.* **65,** 1302–1305
29. Luo, X., and Yu, H. (2008) Protein metamorphosis. The two-state behavior of Mad2. *Structure* **16,** 1616–1625

30. Okada, T., Sonoda, E., Yoshimura, M., Kawano, Y., Saya, H., Kohzaki, M., and Takeda, S. (2005) Multiple roles of vertebrate REV genes in DNA repair and recombination. *Mol. Cell. Biol.* **25,** 6103–6111
31. Bomar, M. G., Pai, M. T., Tzeng, S. R., Li, S. S., and Zhou, P. (2007) Structure of the ubiquitin-binding zinc finger domain of human DNA Y-polymerase η. *EMBO Rep.* **8,** 247–251
32. Bomar, M. G., D'Souza, S., Bienko, M., Dikic, I., Walker, G. C., and Zhou, P. (2010) Unconventional ubiquitin recognition by the ubiquitin-binding motif within the Y family DNA polymerases ι and Rev1. *Mol. Cell* **37,** 408–417
33. Cui, G., Benirschke, R. C., Tuan, H. F., Juranić, N., Macura, S., Botuyan, M. V., and Mer, G. (2010) Structural basis of ubiquitin recognition by translesion synthesis DNA polymerase ι. *Biochemistry* **49,** 10198–10207
34. Burschowsky, D., Rudolf, F., Rabut, G., Herrmann, T., Peter, M., Matthias, P., and Wider, G. (2011) Structural analysis of the conserved ubiquitin-binding motifs (UBMs) of the translesion polymerase ι in complex with ubiquitin. *J. Biol. Chem.* **286,** 1364–1373
35. Hendel, A., Krijger, P. H., Diamant, N., Goren, Z., Langerak, P., Kim, J., Reissner, T., Lee, K. Y., Geacintov, N. E., Carell, T., Myung, K., Tateishi, S., D'Andrea, A., Jacobs, H., and Livneh, Z. (2011) PCNA ubiquitination is important, but not essential for translesion DNA synthesis in mammalian cells. *PLoS Genet.* **7,** e1002262
36. Edmunds, C. E., Simpson, L. J., and Sale, J. E. (2008) PCNA ubiquitination and REV1 define temporally distinct mechanisms for controlling translesion synthesis in the avian cell line DT40. *Mol. Cell* **30,** 519–529
37. Lawrence, C. W., and Christensen, R. B. (1979) Ultraviolet-induced reversion of cyc1 alleles in radiation-sensitive strains of yeast. III. rev3 mutant strains. *Genetics* **92,** 397–408
38. Lawrence, C. W., and Christensen, R. B. (1982) The mechanism of untargeted mutagenesis in UV-irradiated yeast. *Mol. Gen. Genet.* **186,** 1–9
39. D'Souza, S., and Walker, G. C. (2006) Novel role for the C terminus of *Saccharomyces cerevisiae* Rev1 in mediating protein-protein interactions. *Mol. Cell. Biol.* **26,** 8173–8182
40. Acharya, N., Haracska, L., Johnson, R. E., Unk, I., Prakash, S., and Prakash, L. (2005) Complex formation of yeast Rev1 and Rev7 proteins. A novel role for the polymerase-associated domain. *Mol. Cell. Biol.* **25,** 9734–9740
41. Acharya, N., Johnson, R. E., Prakash, S., and Prakash, L. (2006) Complex formation with Rev1 enhances the proficiency of *Saccharomyces cerevisiae* DNA polymerase ζ for mismatch extension and for extension opposite from DNA lesions. *Mol. Cell. Biol.* **26,** 9555–9563
42. Deans, A. J., and West, S. C. (2011) DNA interstrand cross-link repair and cancer. *Nat. Rev. Cancer* **11,** 467–480
43. Ho, T. V., and Schärer, O. D. (2010) Translesion DNA synthesis polymerases in DNA interstrand cross-link repair. *Environ. Mol. Mutagen.* **51,** 552–566
44. Lin, X., Okuda, T., Trang, J., and Howell, S. B. (2006) Human REV1 modulates the cytotoxicity and mutagenicity of cisplatin in human ovarian carcinoma cells. *Mol. Pharmacol.* **69,** 1748–1754
45. Okuda, T., Lin, X., Trang, J., and Howell, S. B. (2005) Suppression of hREV1 expression reduces the rate at which human ovarian carcinoma cells acquire resistance to cisplatin. *Mol. Pharmacol.* **67,** 1852–1860
46. Xie, K., Doles, J., Hemann, M. T., and Walker, G. C. (2010) Error-prone translesion synthesis mediates acquired chemoresistance. *Proc. Natl. Acad. Sci. U. S. A.* **107,** 20792–20797
47. Doles, J., Oliver, T. G., Cameron, E. R., Hsu, G., Jacks, T., Walker, G. C., and Hemann, M. T. (2010) Suppression of Rev3, the catalytic subunit of Polζ, sensitizes drug-resistant lung tumors to chemotherapy. *Proc. Natl. Acad. Sci. U. S. A.* **107,** 20786–20791